Available online at www.sciencedirect.com
SCIENCE DIRECT®
Bioorganic & Medicinal Chemistry Letters
Bioorganic & Medicinal Chemistry Letters 15 (2005) 4671–4680

Density-functional theory studies on standard electrode potentials of half reaction for L-adrenaline and adrenalinequinone

Yuanzhi Song,[a,*] JianFeng Zhou,[a] Yang Song,[b] Yongge Wei[c] and Hong Wang[d]

[a]*Chemistry Department, Huaiyin Teachers College, Jiangsu Province Key Laboratory for Chemistry of Low-Dimensional Materials, Huai An 223300, People's Republic of China*
[b]*College of Materials Science and Engineering, Beijing University of Chemical Technology, Peking 100029, People's Republic of China*
[c]*Chemistry Department, Peking University, Peking 100871, People's Republic of China*
[d]*Medical College, Wuhan University, Wuhan 430070, People's Republic of China*

Received 30 April 2005; revised 29 July 2005; accepted 29 July 2005
Available online 13 September 2005

Abstract—DFT (B3LY/6-31G(d) and B3PW91/6-31G(d)) calculations are performed for L-adrenaline and adrenalinequinone. The calculated IR spectrum of L-adrenaline is used for the assignment of IR frequencies that are observed in the experimental IR spectrum. Cyclic voltammetry with a platinum electrode of L-adrenaline solutions in phosphate buffers at pH 1 shows that standard electrode potential of half reaction for L-adrenaline and adrenalinequinone is 0.803 V. Standard electrode potential of half reaction for L-adrenaline and adrenalinequinone is calculated using the energies of solvation and the sum of electronic and thermal free energies of L-adrenaline and adrenalinequinone.

L-Adrenaline is known to be an important hormone secreted by the medulla of the adrenal gland, which also serves as a chemical mediator for conveying the nerve pulse to efferent organs. Numerous observations on electrochemical behavior of catechols and its analogs, such as epinephrine, often called L-adrenaline, have been carried out in many research groups.[1–10]

Standard electrode potential is a very important parameter in biochemistry, analytical chemistry, etc. Therefore, the prediction of standard electrode potential is very important. The previous paper[11] gave literature values of standard Gibbs energies of formation ($\Delta_f G^0$) and standard enthalpies of formation ($\Delta_f H^0$) for 72 species involved in enzyme-catalyzed reactions. These values were used to calculate standard transformed Gibbs energies of formation ($\Delta_f G'^0$) and standard transformed enthalpies of formation ($\Delta_f H'^0$) for reactants (sum of species) at 298.15 K, pH 7. Some of the $\Delta_f G^0$ and $\Delta_f H^0$ values were obtained from the literature,[12] while the others were derived from the interpretation of apparent equilibrium constants (K') of biochemical reactions where the acid dissociation constants were known for all the reactants. The previous article[13] attempted to include all the literature data on the species of interest in biochemical reactions because its objective was to show how $\Delta_f G^0$ and $\Delta_f H^0$ values for species could be used to calculate $\Delta_f G'^0$ and $\Delta_f H'^0$ values for reactants at pH 7 and to demonstrate the calculation of apparent equilibrium constants (K') at pH 7. The $\Delta_f G'^0$ values calculated from $\Delta_f G^0$ values were tested by calculating apparent equilibrium constants for reactions for which there are good experimental data. Since that test was satisfactory, the $\Delta_f G'^0$ values were then used to calculate the standard transformed Gibbs energy of reaction values for 11 more reactants by use of experimental K' values for reactions. These new $\Delta_f G'^0$ values are calculated using

$$\Delta_r G^0 = -RT \ln K' = \sum v'_i \Delta_f G'^0_i,$$

where $\Delta_r G^0$ is the standard transformed Gibbs energy of the reaction of the reactant i at pH 7 and v'_i is the stoichiometric number of reactant i (positive for products and negative for reactants) in the biochemical reaction.

The standard transformed Gibbs energy of reaction is also related to standard electrode potential. Thus, the

Keywords: L-Adrenaline; Adrenalinequinone; DFT; IR spectrum; Cyclic voltammetry; Standard electrode potential.
* Corresponding author. Tel.: +86 517 3766342; fax: +86 517 4926385; e-mail: songyuanzhi@sina.com.cn

0960-894X/$ - see front matter © 2005 Elsevier Ltd. All rights reserved.
doi:10.1016/j.bmcl.2005.07.084

theoretical calculation of standard electrode potential is significant.

Figure 1 shows the reaction scheme for the L-adrenaline case. The oxidation of L-adrenaline at a relatively low hydrogen ion concentration represents an example of the so-called ECC mechanism[14,15] (which shows that an electrode reaction follows a chemical reaction).

In this paper, the vibrational frequencies for L-adrenaline are calculated for validation of the structure because the molecular parameters are controlled by the structure; furthermore, standard electrode potential of half reaction for L-adrenaline and adrenalinequinone is also calculated using the optimized structure at the same level.

Many study results have indicated that density-functional theory is a powerful method for predicting the geometry and hormonic vibration of organic compounds.[16–20] Therefore, the DFT-B3LYP/6-31G(d) and DFT-B3PW91/6-31G(d) were carried out to study the molecular structure, solvation energies, sum of electronic and thermal free energies, and the vibrational frequencies of both L-adrenaline and its oxidized form (adrenalinequinone) at electrode (Fig. 2).

The DFT calculations (B3LYP and B3PW91[21]) were performed using the 6-31G(d) basis set with Gaussian 98 program.[22] The geometry optimizations of investigated L-adrenaline and adrenalinequinone were performed under relaxation of all internal degrees of freedom, assuming planarity of benzene ring of the molecules (Cs symmetry). The harmonic vibrational frequencies, as well as infrared intensities, were subsequently calculated by using the numerical differentiation of analytical gradients. The visualization of atom movement was made possible by using the gaussView2.1.[23] The energies of solvation of L-adrenaline and adrenalinequinone at 298.15 K, 1 atm were calculated by the Polarized Continuum (overlapping spheres) model (PCM) of Tomasi and co-workers for analytic energies at the same levels.[24–26]

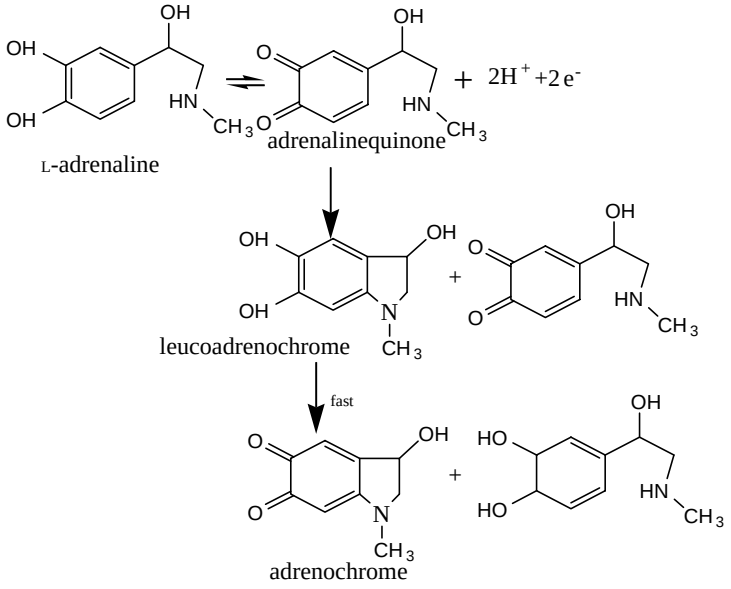

Figure 1. Reaction scheme for the electrochemical oxidation of L-adrenaline.

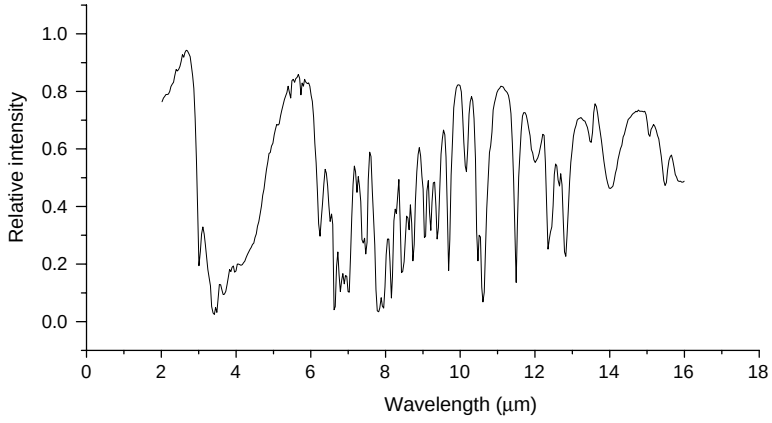

Figure 2. The IR spectrum of L-adrenaline.

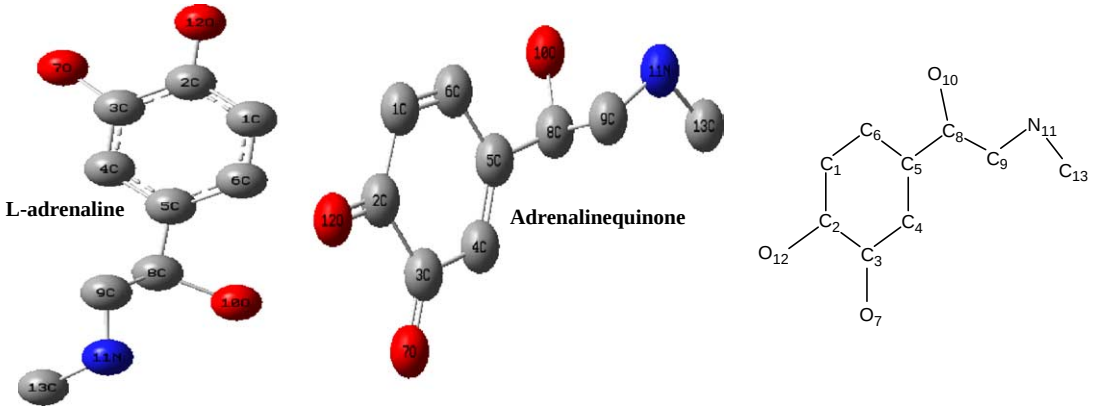

Figure 3. Numbering in both L-adrenaline and adrenalinequinone and geometries of L-adrenaline and adrenalinequinone optimized at the B3LYP/6-31G(d) level.

The geometries and numeration of atoms in both L-adrenaline and adrenalinequinone are shown in Figure 3. All atoms of the benzene ring with OH and O atoms in both L-adrenaline and adrenalinequinone are in planar configuration.

The bond lengths and bond angles of both L-adrenaline and adrenalinequinone optimized at the BLYP/6-31G(d) and B3PW91/6-31G(d) levels are given in Table 1. It can be seen from Table 1 that the bond lengths and bond angles of the same molecule at the BLYP/6-31G(d) level are in good agreement with that at the B3PYW91/6-31G(d) level. From Table 1 the band lengths of C_3C_7 and C_2C_{12} in adrenalinequinone are shorter than in L-adrenaline because of the form of two carbonyls; however, the band lengths of C_3C_4, C_5C_6, and C_1C_2 in adrenalinequinone are longer than in L-adrenaline. So, the bond angles of $C_4C_5C_6$, $C_5C_6C_1$, $C_5C_6C_1$, and $C_1C_2C_3$, as well as the dihedral angles of $C_4C_5C_8C_9$, $C_6C_5C_8C_9$, $C_{10}C_8C_9C_{11}$, $C_4C_5C_8C_{10}$, and $C_6C_5C_8C_{10}$ also change markedly with the changes in bond lengths.

Because adrenalinequinone, as an intermediate in an electrode process, is unstable, only an experimental spectrum of L-adrenaline is shown in Figure 2. The ordinate is the IR relative intensity, while the abscissa represents the frequency (cm^{-1}). The calculated vibrational spectrum shows that there are systematic errors between predicted bonds and experimental spectrum. Scaling of the force constants according to the methods reported by Schaefer III et al.[27] and Paulay et al.[28] is a very useful way to account for systematic errors such as the neglect of harmonic effects, basis set defects, and election correlation. In many cases, the typical values for the scaling factors range from 0.7 to 0.99, while the scaling factors of B3LYP/6-31G(d) and of B3PW91/6-31G(d) are 0.9614 and 0.9753,[29] respectively, for predicting the vibrational spectrum of L-adrenaline. The calculated frequencies and experimental frequencies are shown in Table 2 and Figure 4.

The predicted spectrum for L-adrenaline at the B3LYP/6-31G(d) level gives 72 vibrational modes. The good overall appearance agreement with experimental data for L-adrenaline, particularly for low-frequency modes, confirms the reliability of the presented band assignment. The strongest peak in the calculated spectrum appears at 1274 cm^{-1}, whereas the experimental bond is located at 1282 cm^{-1}; in both cases of experimental and theoretical, the vibration is benzene ring breathing. Three modes are associated with the bands of OH stretching, which are located at 3627, 3575, and 3434 cm^{-1}; however, only a band at 3304 cm^{-1} is found in the experimental spectrum on account of vibration coupling in the solid state. The intensities of $N_{11}H$ stretching in experimental are so weak that they cannot be found in the IR spectrum, the results indicating that errors do exist at higher frequencies between calculated spectrum and experimental frequencies.[30] Four modes refer to the bands of CH stretching, which appeared at 2832, 2871, 3010, and 3030 cm^{-1} in the predicted spectrum but were located at 2800, 2872, 2916, and 2974 cm^{-1} in the IR spectrum. Modes 32, 33, 35, 57, and 59 were assigned to the bands of CC stretching, which were located at 931, 1008, 1086, 1517, and 1613 cm^{-1}, whereas they appear at 939, 1010, 1082, 1532, and 1610 cm^{-1} in the IR spectrum, respectively. The region from 612 to 1485 cm^{-1} in a predicted spectrum mainly represents the bands of CH rock and NH rocks, benzene ring torsion, benzene ring breathing, and CC bond bending, which are in good agreement with that observed in the IR spectrum.

In adrenalinequinone, the frequencies of OH and NH stretching in the predicted spectrum at the B3LYP/6-31G(d) level are located at 3395 and 3398 cm^{-1}, while the bands of CO stretching appear at 1687 and 1685 cm^{-1}. Modes 64, 63, and 62 represent the bands of CH stretching in the benzene ring, which are located at 3083, 3071, and 3104 cm^{-1}. The frequencies of CH stretching of methyl and methylene appear at 3017, 2978 and 2973, 2887, 2871 cm^{-1}, respectively.

The predicted frequencies for L-adrenaline and adrenalinequinone at the B3PYW91/6-31G(d) level are slightly higher than at the B3LYP/6-31G(d) level.

Thus, the structures optimized at the B3LYP/6-31G(d) and B3PYW91/6-31G(d) level are reliable and reasonable.

Table 1. The geometry parameters of L-adrenaline and adrenalinequinone

	L-Adrenaline		Adrenalinequinone	
	B3LYP/6-31G(d)	B3PYW91/6-31G(d)	B3LYP/6-31G(d)	B3PYW91/6-31G(d)
Bond length (Å)				
r (2–12)	1.366	1.360	1.219	1.217
r (3–7)	1.381	1.374	1.220	1.218
r (8–10)	1.416	1.409	1.413	1.405
r (9–11)	1.467	1.460	1.463	1.456
r (1–2)	1.392	1.390	1.473	1.470
r (2–3)	1.405	1.403	1.559	1.555
r (3–4)	1.390	1.388	1.469	1.466
r (4–5)	1.402	1.400	1.354	1.353
r (5–6)	1.397	1.395	1.469	1.466
r (1–6)	1.397	1.395	1.349	1.348
r (5–8)	1.515	1.511	1.512	1.508
r (8–9)	1.548	1.544	1.555	1.551
r (9–11)	1.467	1.460	1.463	1.456
r (11–13)	1.462	1.456	1.464	1.458
Bond angle (°)				
α (12–2–3)	120.5	120.4	120.0	120.0
α (2–3–7)	115.0	114.9	119.9	119.8
α (7–3–4)	124.5	124.6	123.0	123.0
α (4–5–6)	118.8	118.9	121.0	121.0
α (5–6–1)	120.8	120.8	122.7	122.7
α (1–2–3)	119.1	119.1	116.8	116.9
α (4–5–8)	120.0	120.1	121.3	121.3
α (5–8–10)	110.6	110.9	110.3	110.6
α (10–8–9)	108.4	108.2	108.8	108.6
α (5–8–9)	111.2	110.9	110.6	110.2
α (8–9–11)	109.8	109.5	108.9	108.6
α (9–11–13)	114.6	114.6	114.8	114.8
Dihedral angle (°)				
D (6,1,2,12)	−179.9	−179.5	179.5	179.4
D (6,1,2,3)	−0.4	−0.4	−0.5	−0.5
D (4,5,8,9)	−85.8	−85.6	−92.3	−93.3
D (4,5,8,10)	154.0	153.5	147.7	146.4
D (6,5,8,9)	91.7	91.2	85.1	84.1
D (6,5,8,10)	−28.6	−29.0	−34.9	−36.2
D (5,8,9,11)	−168.8	−169.6	−165.9	−167.0
D (10,8,9,11)	−47.0	−47.5	−44.6	−45.8
D (8,9,11,13)	−84.1	−84.3	−84.8	−85.1

The highest occupied molecular orbital (HOMO), the lowest unoccupied molecular orbital (LUMO), and the energy gap of HOMO and LUMO for L-adrenaline and adrenalinequinone calculated at the B3LYP/6-31G(d) and B3PYW91/6-31G(d) levels are shown in Table 3 and Figure 5.

The eigenvalues of LUMO and HOMO and their energy gap reflect the chemical activity of the molecule. LUMO as an electron acceptor represents the ability to obtain an electron, while HOMO as an electron donor represents the ability to donate an electron. The smaller the energy gap of LUMO and HOMO, the easier it is for the electrons of HOMO to be excited; the higher the energies of HOMO, the easier it is for HOMO to donate electrons; the lower the energies of LUMO, the easier it is for LUMO to accept electrons.

From Table 3 and Figure 5, the results show that the energies of LUMO of adrenalinequinone are lower than that of L-adrenaline and the energy gap of adrenalinequinone is smaller than that of L-adrenaline; therefore, transfer of electrons from HOMO to LUMO in adrenalinequinone is relatively easier than that in L-adrenaline, and the LUMO in adrenalinequinone accepts electrons easily with the decrease of the energies of LUMO. As a result, the oxidation of L-adrenaline at a relatively low hydrogen ion concentration represents an example of the so-called ECC mechanism.

Voltammograms for the oxidation of 5.0 mM L-adrenaline in 0.1 M phosphate buffer at pH 1.0 are shown in Figure 6 at a platinum microelectrode. Similar data are obtained at a glassy carbon microelectrode. The voltammograms obtained at a relatively high hydrogen ion concentration (low pH) exhibit a chemically reversible oxidation process, as indicated by similar-sized peaks for the forward and reverse scans, with an oxidation peak potential (E^{ox}) of 0.66 V and a reduction peak potential (E^{red}) of 0.44 V at pH 1.0 versus Ag/AgCl. Compared with previous work, the results are in agreement with the

Table 2. Experimental (υ_{exp}) and calculated (υ_{cal}) vibrational wavenumbers (cm^{-1}), IR absorption intensities (I, km/mol)

Mode	L-Adrenaline					Adrenalinequinone			
	υ_{cal} (cm^{-1}) (I)		υ_{cal} (cm^{-1}) (I)		υ_{exp} (cm^{-1})[33]	υ_{cal} (cm^{-1}) (I)		υ_{cal} (cm^{-1}) (I)	
	B3PYW91/6-31G(d)		B3LYP/6-31G(d)			B3PYW91/6-31G(d)		B3LYP/6-31G(d)	
	Unscaled	Scaled	Unscaled	Scaled		Unscaled	Scaled	Unscaled	Scaled
1	34(1.1)	33	34(1.1)	33		37(1.8)	36	38(1.8)	37
2	61(0.2)	59	61(0.2)	59		56(2.5)	55	56(2.5)	54
3	73(0.6)	71	74(0.6)	71		68(0.7)	66	67(0.7)	64
4	113(1.2)	110	113(1.2)	109		93(0.2)	91	96(0.2)	92
5	174(8.4)	170	174(12.0)	167		121(2.1)	118	121(2.1)	116
6	200(0.5)	195	200(3.6)	192		193(1.3)	188	195(1.1)	187
7	207(41.7)	202	205(77.6)	197		209(7.4)	204	210(5.8)	202
8	213(117.2)	208	210(72.3)	202		213(1.7)	208	215(3.5)	207
9	255(0.8)	249	254(0.5)	244		290(3.2)	283	291(3.7)	280
10	303(5.3)	297	305(5.0)	293		329(7.3)	321	325(6.7)	312
11	324(9.8)	316	319(9.3)	307		346(2.7)	337	345(2.9)	332
12	333(7.8)	325	331(7.3)	318		349(10.2)	340	350(9.2)	336
13	390(5.7)	380	391(4.8)	376		408(1.6)	398	410(1.3)	394
14	422(5.9)	411	422(1.9)	406		448(2.6)	437	450(2.8)	433
15	435(61.2)	424	429(64.8)	412		474(0.7)	462	476(1.0)	458
16	452(18.0)	441	452(12.7)	435		547(12.1)	533	545(12.8)	524
17	469(6.0)	457	469(4.0)	451		579(11.7)	565	579(9.6)	557
18	554(5.8)	540	551(6.3)	530		604(8.1)	589	605(4.4)	582
19	597(31.6)	582	596(30.2)	573		617(9.8)	602	615(11.8)	591
20	617(9.0)	602	612(35.3)	588		675(75.0)	658	653(77.5)	628
21	630(11.2)	603	630(16.3)	606		704(12.8)	687	698(13.6)	671
22	654(62.9)	638	637(36.3)	612	619	768(65.2)	749	765(64.6)	735
23	705(1.2)	688	704(1.0)	677	695	788(11.4)	769	788(8.6)	758
24	772(85.2)	753	769(84.7)	739	733	809(13.4)	789	808(13.4)	777
25	802(12.9)	782	798(12.7)	767	776	833(36.3)	812	834(31.7)	802
26	817(8.0)	797	816(7.1)	784		906(2.8)	884	904(14.3)	869
27	838(1.3)	817	839(2.0)	807	808	915(24.5)	892	911(18.9)	876
28	842(46.8)	821	843(38.5)	810	836	938(2.5)	915	934(1.5)	898
29	914(46.5)	891	907(51.5)	872	873	953(11.5)	929	942(9.0)	906
30	945(2.6)	922	936(1.8)	900		1024(0.17)	999	1024(0.3)	984
31	956(2.6)	932	954(1.2)	917		1024(19.9)	999	1039(20.5)	999
32	973(5.1)	949	968(5.5)	931	939	1116(14.3)	1088	1105(15.1)	1062
33	1049(10.0)	1023	1046(10.9)	1008	1010	1139(12.7)	1111	1133(9.5)	1089
34	1119(80.7)	1091	1110(65.7)	1058	1059	1161(6.0)	1132	1151(46.0)	1107
35	1134(8.5)	1105	1130(29.1)	1086	1082	1167(33.0)	1138	1163(13.2)	1118
36	1162(17.9)	1133	1151(38.4)	1106	1102	1184(24.2)	1155	1177(55.9)	1132
37	1170(33.4)	1141	1167(16.9)	1121		1188(55.5)	1159	1184(19.1)	1138
38	1182(90.6)	1150	1178(38.0)	1132	1130	1206(37.6)	1176	1199(12.7)	1153
39	1192(30.6)	1162	1186(76.7)	1140	1141	1285(34.7)	1253	1282(100.0)	1233
40	1199(17.3)	1169	1192(11.5)	1145		1291(96.4)	1259	1287(30.7)	1237
41	1232(78.5)	1201	1229(75.9)	1182	1180	1314(1.6)	1281	1313(2.8)	1263
42	1284(44.5)	1252	1284(55.3)	1234	1216	1344(5.6)	1311	1394(5.3)	1340
43	1301(27.4)	1256	1296(70.3)	1246		1379(47.6)	1345	1379(50.0)	1326
44	1315(70.9)	1282	1314(69.1)	1263	1257	1392(17.2)	1358	1396(17.7)	1342
45	1338(237.2)	1305	1326(178.9)	1274	1282	1441(54.8)	1405	1440(51.2)	1384
46	1357(4.0)	1310	1356(13.7)	1303		1463(72.0)	1427	1461(67.4)	1405
47	13849(89.3)	1349	1384(95.7)	1330	1338	1478(11.8)	1441	1482(4.7)	1425
48	1393(8.7)	1358	1396(2.5)	1342		1498(2.4)	1461	1450(2.3)	1394
49	1438(27.3)	1315	1425(26.3)	1370	1379	1508(5.4)	1471	1514(2.9)	1456
50	1465(55.4)	1429	1463(67.2)	1400	1420	1522(18.5)	1484	1526(14.8)	1467
51	1478(24.0)	1441	1481(11.9)	1425		1541(8.8)	1503	1545(7.7)	1485
52	1497(26.5)	1460	1494(87.9)	1436	1440	1645(12.7)	1604	1631(11.8)	1568
53	1499(62.2)	1462	1499(6.4)	1441		1707(14.4)	1665	1698(12.9)	1632
54	1507(18.6)	1469	1513(6.4)	1454	1448	1773(263.2)	1729	1755(255.1)	1687
55	1522(17.9)	1484	1525(13.5)	1466	1446	1800(48.6)	1756	1784(47.4)	1715
56	1541(8.2)	1503	1545(7.3)	1485	1488	2994(30.2)	2920	2986(29.6)	2871
57	1587(123.4)	1447	1578(106.6)	1517	1532	3006(69.4)	2932	2994(21.5)	2878
58	1678(26.4)	1636	1666(24.4)	1601	1610	3015(42.0)	2940	3003(52.4)	2887
59	1692(17.3)	1650	1678(17.1)	1613		3105(21.3)	3028	3092(52.3)	2973
60	2953(57.0)	2880	2946(56.1)	2832	2800	3111(26.4)	3034	3098(28.2)	2978
61	2990(66.7)	2916	2978(56.4)	2863		3153(23.3)	3075	3138(25.6)	3017

(*continued on next page*)

Table 2 (*continued*)

Mode	L-Adrenaline					Adrenalinequinone			
	υ_{cal} (cm^{-1}) (*I*)		υ_{cal} (cm^{-1}) (*I*)		υ_{exp} (cm^{-1})[33]	υ_{cal} (cm^{-1}) (*I*)		υ_{cal} (cm^{-1}) (*I*)	
	B3PYW91/6-31G(d)		B3LYP/6-31G(d)			B3PYW91/6-31G(d)		B3LYP/6-31G(d)	
	Unscaled	Scaled	Unscaled	Scaled		Unscaled	Scaled	Unscaled	Scaled
62	2997(67.7)	2923	2986(79.8)	2871	2872	3203(4.4)	3124	3194(5.1)	3071
63	3103(29.5)	3026	3091(31.6)	2972		3216(0.5)	3137	3207(1.1)	3083
64	3109(20.4)	3035	3097(22.2)	2977		3233(5.6)	3153	3226(5.9)	3104
65	3146(26.8)	3068	3131(30.3)	3010	2916	3523(232.7)	3436	3531(126.9)	3395
66	3161(17.6)	3082	3152(19.0)	3030	2974	3565(2.4)	3477	3534(70.4)	3398
67	3219(6.3)	3139	3209(7.6)	3085					
68	3240(2.7)	3160	3231(3.1)	3106					
69	3558(5.8)	3470	3525(0.6)	3389					
70	3571(165.2)	3483	3573(136.7)	3435	3304				
71	3747(90.6)	3654	3719(81.9)	3575					
72	3810(58.5)	3716	3773(50.6)	3627					

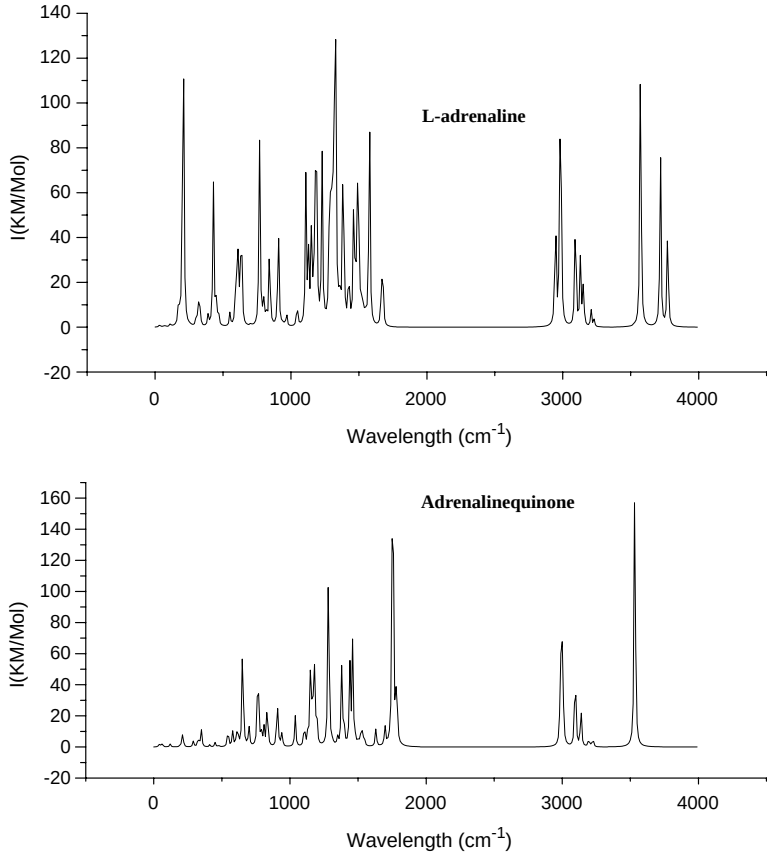

Figure 4. The theoretical spectrum of L-adrenaline and adrenalinequinone at the B3LYP/6-31G(d) level; the wavelength is not scaled.

Table 3. The eigenvalues of LUMO and HOMO and energy gaps of HOMO and LUMO

	E_{HOMO} (eV)		E_{LUMO} (eV)		$E_{LUMO}-E_{HOMO}$ (eV)	
	B3LYP	B3PYW91	B3LYP	B3PYW91	B3LYP	B3PYW91
L-Adrenaline	−5.41	−5.47	0.29	0.24	5.70	5.71
Adrenalinequinone	−6.53	−6.56	−3.32	−3.41	3.21	3.24

literature.[1,3,6] Thus, the conditional potential $E = (E^{ox} + E^{red})/2$;[31] therefore

$$\mathrm{pH} = 1.0, E = (0.66\ \mathrm{V} + 0.44\ \mathrm{V})/2 = 0.550\ \mathrm{V}.$$

So, the standard electrode potential (E_1^o) versus Ag/AgCl can be written as

E is calculated as

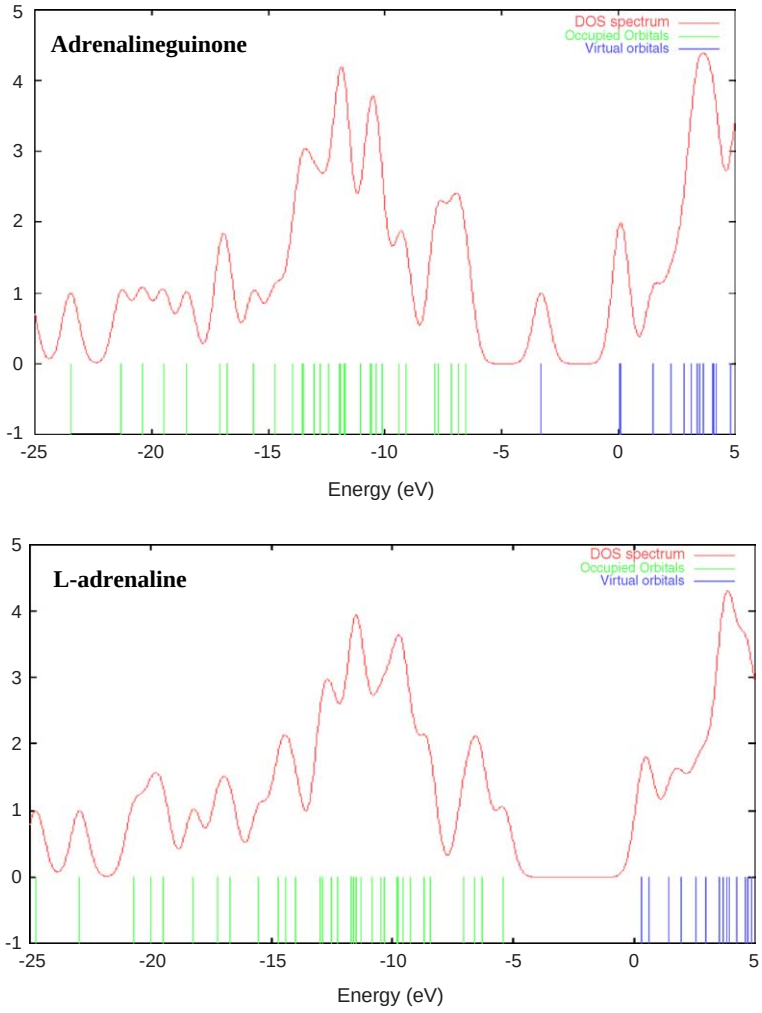

Figure 5. The eigenvalues of LUMO and HOMO of adrenalinequinone and L-adrenaline at the 6-31G(d) level.

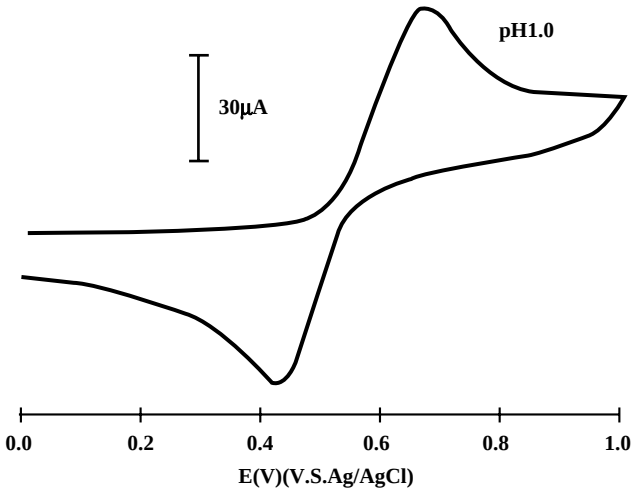

Figure 6. Voltammograms for the oxidation of 5.0 mM L-adrenaline in 0.1 M phosphate at pH 1.0. The voltammograms are obtained in a stationary solution with a 0.8 mm radius platinum disk as a working electrode and using a potential scan rate of 0.1 V s^{-1}.

$$E = E_1^{o} + 0.059\,\lg[H^+]\ (25\ ^{\circ}C).$$

Then

$$pH = 1.0, E_1^{o} = 0.609\ V\ (25\ ^{\circ}C).$$

Standard electrode potential (E_2^{o}) versus normal hydrogen electrode (NHE) is given as

$$E_2^{o} = E_1^{o} + E_{Ag/AgCl(3M\ KCl)},$$

$$\begin{aligned} E_{Ag/AgCl(3M\ KCl)} &= E^{o}_{AgCl/Ag} - 0.059\,\lg[Cl^-] \\ &= 0.222\ V - 0.059\,\lg[3] \\ &= 0.194\ V\ (25\ ^{\circ}C), \end{aligned}$$

where $E^{o}_{AgCl/Ag}$ represents the standard electrode potential for Ag/AgCl;[32] therefore, E_2^{o} is calculated as

$$pH = 1.0, E_2^{o} = 0.609\ V + 0.194\ V = 0.803\ V\ (25\ ^{\circ}C).$$

Half reactions for L-adrenaline and adrenalinequinone, as well as normal hydrogen electrode (NHE), can be written as

$$Adrenalinequinone_{(g)} + 2e^- + 2H^+_{(g)} = L\text{-}adrenaline_{(g)},$$

$$2e^- + 2H^+_{(g)} = H_2(g).$$

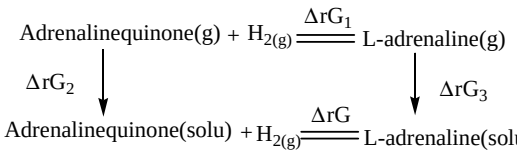

Figure 7. Design of redox reaction of L-adrenaline and adrenalinequinone in solution; g and solu denote gas and solution, respectively.

Then

$$\text{Adrenalinequinone}_{(g)} + \text{H}_{2_{(g)}} = \text{L-adrenaline}_{(g)}. \quad (1)$$

The transformed Gibbs energy of (1) is written as

$$\begin{aligned}\Delta_r G_1(298.15\,\text{K}) &= G_{\text{L-adrenaline}} - G_{\text{Adrenalinequinone}} - G_{\text{H}_2} \\ &= (\varepsilon_0 + G_{\text{corr}})_{\text{L-adrenaline}} \\ &\quad - (\varepsilon_0 + G_{\text{corr}})_{\text{Adrenalinequinone}} - (\varepsilon_0 + G_{\text{corr}})_{\text{H}_2}.\end{aligned}$$

The redox reaction in solution was designed as in Figure 7.

So, the standard transformed Gibbs energy of reaction in solution is written as

$$\Delta_r G(298.15\,\text{K}, 1\,\text{atm}) = \Delta_r G_1 - \Delta_r G_2 + \Delta_r G_3,$$

where $\Delta_r G_2$ and $\Delta_r G_3$ are energies of solvation of adrenalinequinone and L-adrenaline in water at 298.15 K, 1 atm, respectively. G_{corr} is given as

$$G_{\text{corr}} = H_{\text{corr}} - TS_{\text{tot}},$$

$$H_{\text{corr}} = E_{\text{tot}} + k_B T,$$

$$S_{\text{tot}} = S_t + S_r + S_v + S_{e^-},$$

The Gibbs free energy includes $\Delta PV = \Delta NRT$, so when it is applied to calculated $\Delta_r G$ for a reaction, $\Delta NRT = \Delta PV$ is already included. This means that $\Delta_r G$ will be computed correctly when the number of moles of gas changes during the course of a reaction. The next equations are estimates of the total energy of the molecule, which is written as

$$\begin{aligned}&\text{sum of electronic and zero-point energies} = \varepsilon_0 + \varepsilon_{\text{ZPE}}, \\ &\text{sum of electronic and thermal energies} = \varepsilon_0 + E_{\text{tot}}, \\ &\text{sum of electronic and thermal enthalpies} = \varepsilon_0 + H_{\text{corr}}, \\ &\text{sum of electronic and thermal free energies} = \varepsilon_0 + G_{\text{corr}}.\end{aligned}$$

Standard electrode potential (E^o) of half reaction for L-adrenaline and adrenalinequinone is calculated as

$$\Delta_r G(298.15\,\text{K}) = -nFE^o.$$

The physical means of descriptor mentioned above is listed in Table 4.

Calculated thermochemistry values from Gaussian 98 for reaction (1) are given in Table 5. The $\Delta_r G(298.15\,\text{K})$ for reaction (1) and standard electrode potential (E^o) of half reaction for L-adrenaline and adrenalinequinone are also calculated. The zero-point energies (ε_{ZPE}) of L-adrenaline and adrenalinequinone are scaled by 0.9614 at the B3LYP/6-31G(d) and 0.9753 at B3PW91/6-31D(d) levels, respectively. From Table 4 all energies, the transformed Gibbs energy of reaction (1) and standard potential calculated at B3LYP/6-31G(d) level, are in agreement with that calculated at the B3PYW91/6-31G(d) level. The predicted standard electrode potentials of 0.57 V at the B3LYP/6-31G(d) level and 0.67 V at the B3PYW91/6-31G(d) level are close to experimental values of 0.802 at pH 1.0. The method at the B3PYW91/6-31G(d) level is superior to that at the B3LYP/6-31G(d) level.

Table 4. Physical mean of descriptor

Descriptor	Physical mean
E_e	Internal energy due to electronic motion
E_r	Internal energy due to rotational motion
E_{tot}	Total internal energy ($E_t + E_r + E_v + E_e$)
E_t	Internal energy due to translation
E_v	Internal energy due to vibrational motion
G_{corr}	Correction to the Gibbs free energy due to internal energy
H_{corr}	Correction to the enthalpy due to internal energy
N	Number of moles
P	Pressure (1 atmosphere)
S_e	Entropy due to electronic motion
S_r	Entropy due to rotational motion
S_{tot}	Total entropy ($S_t + S_r + S_v + S_e$)
S_t	Entropy due to translation
S_v	Entropy due to vibrational motion
T	Temperature (298.15 K)
V	Volume
k_B	Boltzmann constant = 1.380662×10^{-23} J/K
F	Faraday constant = 96.485 C mol^{-1}
ε_{ZPE}	Zero-point energy of the molecule
ε_0	The total electronic energy

The parameters of L-adrenaline and adrenalinequinone are controlled by molecular geometry. The predicted frequencies of L-adrenaline are consistent with the experimental spectrum, indicating that the geometries of L-adrenaline and adrenalinequinone are reasonable and reliable. However, there is an error between the predicted standard potential (0.57 V at the B3LYP/6-31G(d) and 0.67 V at the B3PW91/6-31G(d) levels) and experimental data (0.803 V at pH 1.0). The errors may have arisen from the experimental result and the calculational methods. However, this method is very useful to predict the unknown standard potential of compounds because the theoretical method is very simple and cheap.

Experimental. In Figure 2, the experimental IR spectrum of L-adrenaline in solid state is from the literature.[33]

Phosphate buffers were prepared by titration of analytical reagent grade phosphoric acid with sodium hydroxide until the required pH value reached. A polarograph (Jiangsu Electrochemistry Analysis Instrument Corp., China) with a MEC-12B analytical software is performed for testing the electrochemical behavior. Conventional voltammetric experiments in phosphate buffers were performed at a scan rate of 0.1 V s^{-1} (step width 1 mV) with either a 1.5 mm radius carbon disk or a 0.8 mm radius platinum disk working electrode and a

Table 5. Calculated thermochemistry values, the $\Delta_r G(298.15\,K)$ and standard electrode potential (E^o)

	Adrenalinequinone		H_2		L-Adrenaline	
	B3LYP	B3PYW91	B3LYP	B3PYW91	B3LYP	B3PYW91
ε_0 (Hartree)	−629.937602	−629.697778	−1.175482	−1.174562	−631.175024	630.9410400
ε_{ZPE} (Hartree)	0.193071	0.193654	0.010145	0.010130	0.216490	0.217337
E_{tot} (Hartree)	0.205572	0.206144	0.012505	0.012491	0.229598	0.230403
H_{corr} (Hartree)	0.206516	0.207088	0.013450	0.013435	0.230542	0.231347
G_{corr} (Hartree)	0.153158	0.153720	−0.001342	−0.001358	0.176489	0.177380
$\varepsilon_0 + \varepsilon_{ZPE}$ (Hartree)	−629.744530	−629.504124	−1.165337	−1.164432	−630.958534	−630.723703
$\varepsilon_0 + E_{tot}$ (Hartree)	−629.732030	−629.491634	−1.162977	−1.162071	−630.945426	−630.710637
$\varepsilon_0 + H_{corr}$ (Hartree)	−629.731086	−629.490690	−1.162033	−1.161127	−630.944482	−630.709693
$\varepsilon_0 + G_{corr}$ (Hartree)	−629.784443	−629.544058	−1.176825	−1.175920	−630.998535	−630.763660
$\Delta_r G_1$ (B3LYP) (kJ/mol)			−97.84			
$\Delta_r G_1$(B3PYW91) (kJ/mol)			−114.69			
$\Delta_r G_3$(B3LYP) (kJ/mol)			−65.79			
$\Delta_r G_3$(B3PW91) (kJ/mol)			−70.14			
$\Delta_r G_2$(B3LYP) (kJ/mol)			−53.63			
$\Delta_r G_2$(B3PW91) (kJ/mol)			−55.43			
$\Delta_r G$(B3LYP) (kJ/mol)			−110.00			
$\Delta_r G$(B3PW91) (kJ/mol)			−129.40			
E^o (B3LYP) (V)			0.57			
E^o (B3PYW91) (V)			0.67			

Ag/AgCl (3 M KCl) reference electrode. A platinum wire served as the auxiliary electrode. The working electrode was polished with 5 μm and then 1 μm alumina slurries before each series of experiments.

Acknowledgments

This research was supported by National Youthful Sciences Foundation of China (Grant No. 20302002) and Science Foundation of education department of Jiangsu province of China (Grant No. 04KJD150038).

References and notes

1. Tait, R. J.; Finnin, B. C.; Reed, B. L.; Bond, A. M. *Anal. Chim. Acta* **1996**, *324*, 1.
2. Fike, R. R.; Curran, D. J. *Anal. Chem.* **1977**, *49*, 1205.
3. Hawley, M. D.; Tatawawadi, S. V.; Piekarski, S.; Adams, R. N. *J. Am. Chem. Soc.* **1967**, *89*, 447.
4. Cooper, B. R.; Jankowski, J. A.; Leszczyszyn, D. J.; Wightman, R. M.; Jorgenson, J. W. *Anal. Chem.* **1992**, *64*, 691.
5. Christenson, R. H.; MeGlothlin, C. D. *Anal. Chem.* **1982**, *54*, 2015.
6. Wu, X.; Mu, L.; Zhang, W. *J. Electroanal. Chem.* **1993**, *352*, 295.
7. Sucheta, A.; Rusling, F. *J. Electroanalysis* **1991**, *3*, 735.
8. Deakin, M. R.; Kovach, P. M.; Stutle, K. J.; Wightman, R. M. *Anal. Chem.* **1986**, *58*, 1474.
9. Wightman, R. M.; May, L. J.; Michael, A. C. *Anal. Chem.* **1988**, *60*, 769A.
10. Dryhurst, G. In *Comprehensive Treatise of Electrochemistry*; Plenum Press: New York, 1985; Vol. 10, Chapter 2.
11. Alberty, R. A. *Arch. Biochem. Biophys.* **1998**, *353*, 116.
12. Wagman, D. D.; Evans, W. H.; Parker, V. B.; Schumm, R. H.; Hallow, I.; Bailey, S. M.; Churney, K. L.; Nuttall, R. L. *J. Phys. Chem. Ref. Data* **1982**, *11*(suppl. 2).
13. Alberty, R. A. *Biochem. Biophys. Acta* **1998**, *358*, 25.
14. Hawley, M. D.; Tatawawadi, S. V.; Piekarski, S.; Adams, R. D. *J. Am. Chem. Soc.* **1967**, *89*, 447.
15. Young, T. E.; BaBitto, B. W. *J. Org. Chem.* **1993**, *48*, 562.
16. Scott, P.; Radom, L. *J. Phys. Chem.* **1996**, *100*, 16505.
17. Denis, P.; Ventura, O. N. *J. Mol. Struct.* **2001**, *537*, 173.
18. Abbowicz-Bienko, A. J.; Bienko, D. C.; Latajka, Z. *J. Mol. Struct.* **2000**, *552*, 165.
19. Jacob, R.; Fiscker, G. *J. Mol. Struct.* **2002**, *613*, 175.
20. Banclersen, K.; Langgard, M.; Sparget-Larsen, J. *J. Mol. Struct.* **1999**, *509*, 153.
21. Becke, A. D. *J. Chem. Phys.* **1993**, *98*, 5648.
22. Frisch, M. J.; Trucks, G. W.; Schlegel, H. B.; Scuseria, G. E.; Robb, M. A.; Cheeseman, J. R.; Zakrzewski, V. G.; Montgomery, J. A.; Stratmann, R. E., Jr.; Burant, J. C.; Dapprich, S.; Millam, J. M.; Daniels, A. D.; Kudin, K. N.; Strain, M. C.; Farkas, O.; Tomasi, J.; Barone, V.; Cossi, M.; Cammi, R.; Mennucci, B.; Pomelli, C.; Adamo, C.; Clifford, S.; Ochterski, J.; Petersson, G. A.; Ayala, P. Y.; Cui, Q.; Morokuma, K.; Malick, D. K.; Rabuck, A. D.; Raghavachari, K.; Foresman, J. B.; Cioslowski, J.; Ortiz, J. V.; Baboul, A. G.; Stefanov, B. B.; Liu, G.; Liashenko, A.; Piskorz, P.; Komaromi, I.; Gomperts, R.; Martin, R. L.; Fox, D. J.; Keith, T.; Al-Laham, M. A.; Peng, C. Y.; Nanayakkara, A.; Challacombe, M.; Gill, P. M. W.;

Johnson, B.; Chen, W.; Wong, M. W.; Andres, J. L.; Gonzalez, C.; Head-Gordon, M.; Replogle, E. S.; Pople, J. A.; Gaussian, Inc: Pittsburgh, PA, 1998.
23. GaussView 2.1, Gaussian, Inc.; Carnegie Office Park, Carnegie, PA 15106, USA.
24. Bonaccorsi, R.; Cimiraglia, R.; Tomasi, J. *Comput. Chem.* **1983**, *4*.
25. Pascualahuir, J. L.; Silla, E.; Tomasi, J.; Bonaccorsi, R. J. *Comput. Chem.* **1987**, *8*, 778.
26. Miertus, S.; Scrocco, E.; Tomasi, J. *Chem. Phys.* **1981**, *55*, 117.
27. Yamauchi, Y.; Frisch, M.; Gaw, J.; Schaefer, H. F., III *J. Chem. Phys.* **1986**, *84*, 2262.
28. Pulay, D.; Fogarasi, G.; Pang, F. F.; Boggs, J. E. *J. Am. Chem. Soc.* **1979**, *101*, 2550.
29. Scott, A. P.; Radom, L. *J. Phys. Chem.* **1996**, *100*, 16502.
30. Vladimir, A.; Basiuk, L. *Spectrochim. Acta, Part A* **2001**, *57*, 1271.
31. Wang, J. *Analytical Electrochemistry*, 2nd ed.; John Wiley & Sons: New York, 2000; Chapter 2.
32. Dobos D. Electrochemical Data. New York, 1975.
33. Smith, A. L. The Coblentz Society Desk Book of Infrared Spectra. In *The Coblentz Society Desk Book of Infrared Spectra*, 2nd ed.; Carver, C. D., Ed.; The Coblentz Society: Kirkwood, MO, 1982; pp 1–24.